Lecture notes on Chapter 13: Electron Monte Carlo Simulation

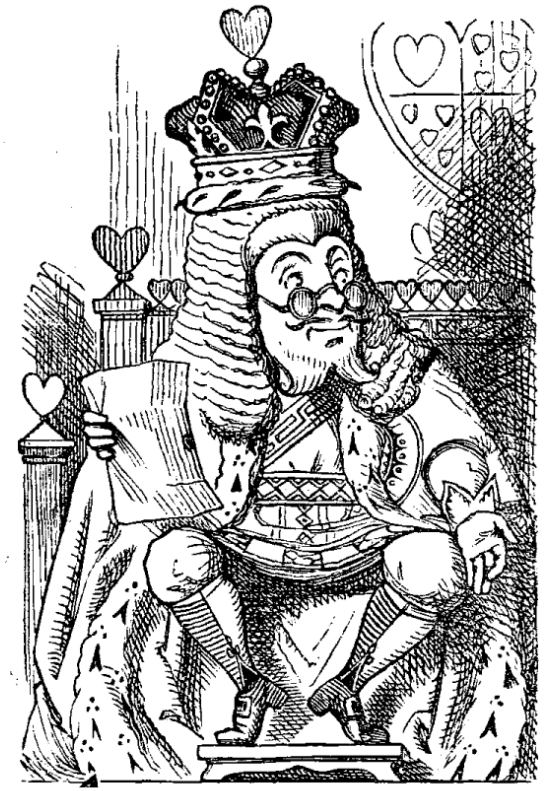

"Begin at the beginning," the King said gravely, "and go on till you come to the end: then stop."

Topics covered

- Basic, relevant interaction processes
- "Hard" or "catastrophic" *vs.* "soft" or "statistically-grouped" interactions
- Basic algorithms of Monte Carlo electron interaction and transport
- Flowchart for an electron Monte Carlo code

Chapter 13: Catastrophic interactions

In this chapter we discuss the electron and positron interactions and discuss the approximations made in their implementation. We give a brief outline of the electron transport logic used in Monte Carlo simulations.

The transport of electrons (and positrons) is considerably more complicated than for photons. Like photons, electrons are subject to violent interactions. The following are the "catastrophic" interactions:

- large energy-loss Møller scattering ($e^- e^- \longrightarrow e^- e^-$),
- large energy-loss Bhabha scattering ($e^+ e^- \longrightarrow e^+ e^-$),
- hard bremsstrahlung emission ($e^{\pm}\mathrm{N} \longrightarrow e^{\pm}\gamma\mathrm{N}$), and
- positron annihilation "in-flight" and at rest ($e^+ e^- \longrightarrow \gamma\gamma$).

It is possible to sample the above interactions discretely in a reasonable amount of computing time for many practical problems.

Chapter 13: Soft, statistically grouped interactions

In addition to the catastrophic events, there are also "soft" events. Detailed modeling of the soft events can usually be approximated by summing the effects of many soft events into virtual "large-effect" events. These "soft" events are:

- low-energy Mølller (Bhabha) scattering (modeled as part of the collision stopping power),
- atomic excitation ($e^{\pm}\mathrm{N} \longrightarrow e^{\pm}\mathrm{N}^{*}$) (modeled as another part of the collision stopping power),
- soft bremsstrahlung (modeled as radiative stopping power), and
- elastic electron (positron) multiple scattering from atoms, ($e^{\pm}\mathrm{N} \longrightarrow e^{\pm}\mathrm{N}$).

Strictly speaking, an elastic large angle scattering from a nucleus should really be considered to be a "catastrophic" interaction but this is not the usual convention. (Perhaps it should be.) For problems of the sort we consider, it is impractical to model all these interactions discretely. Instead, well-established statistical theories are used to describe these "soft" interactions by accounting for them in a cumulative sense including the effect of many such interactions at the same time. These are the so-called "statistically-grouped" interactions.

13.0 Catastrophic interaction threshold

We have almost complete flexibility in defining the threshold between "catastrophic" and "statistically grouped" interactions. The location of this threshold should be chosen by the demands of the physics of the problem and by the accuracy required in the final result.

We will use the symbols Δ_γ and Δ_e to represent the energies forming the boundaries between the soft radiative and soft collision interactions.

This is a long discussion!

13.1.1 Hard bremsstrahlung production ...

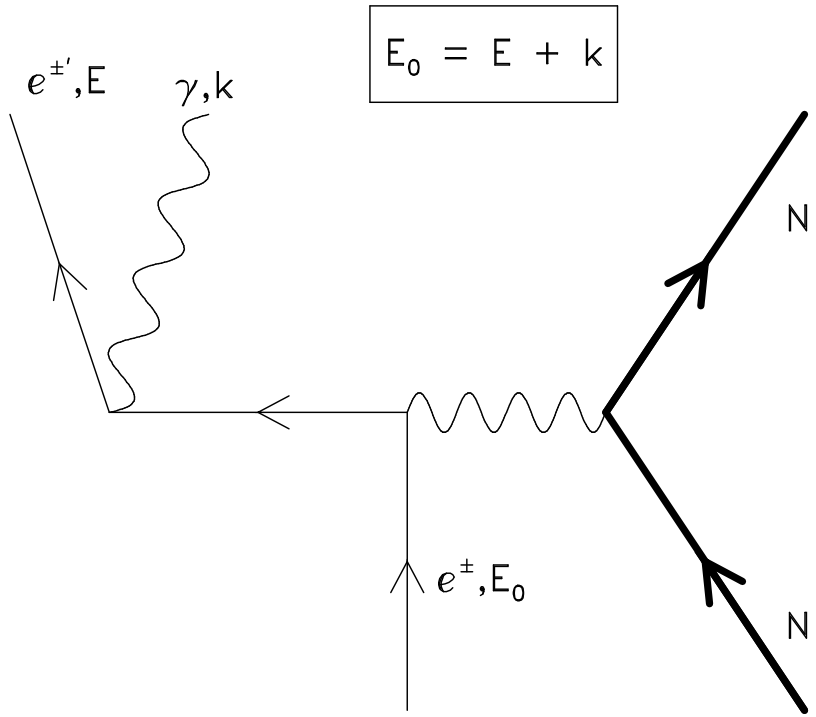

Figure 1: Hard bremsstrahlung production in the field of an atom as depicted by a Feynman diagram. There are two possibilities. The predominant mode (shown here) is a two-body interaction where the nucleus recoils. This effect dominates by a factor of about Z^2 over the three-body case where an atomic electron recoils (not shown).

13.1.1 ... Hard bremsstrahlung production ...

As depicted by the Feynman diagram in above, bremsstrahlung production is the creation of photons by electrons (or positrons) in the field of an atom.

There are actually two possibilities.

The predominant mode is the interaction with the atomic nucleus. This effect dominates by a factor of about Z over the three-body case where an atomic electron recoils ($e^{\pm}\mathrm{N} \longrightarrow e^{\pm}e^{-}\gamma\mathrm{N}^{*}$). Bremsstrahlung is the quantum analogue of synchrotron radiation, the radiation from accelerated charges predicted by Maxwell's equations. The deacceleration and acceleration of an electron scattering from nuclei can be quite violent, resulting in very high energy quanta, up to and including the total kinetic energy of the incoming charged particle.

The two-body effect can be taken into account through the total cross section and angular distribution kinematics.

13.1.1 ... Hard bremsstrahlung production

The three-body case (an atomic electron provides the recoil) is conventionally treated only by inclusion in the total cross section of the two body-process. The two-body process can be modeled using one of the Koch and Motz formulae. The bremsstrahlung cross section scales with $Z(Z + \xi(Z))$, where $\xi(Z)$ is the factor accounting for three-body case where the interaction is with an atomic electron. These factors comes are taken from the work of Tsai. The total cross section depends approximately like $1/E_\gamma$.

13.1.2 Møller (Bhabha) scattering ...

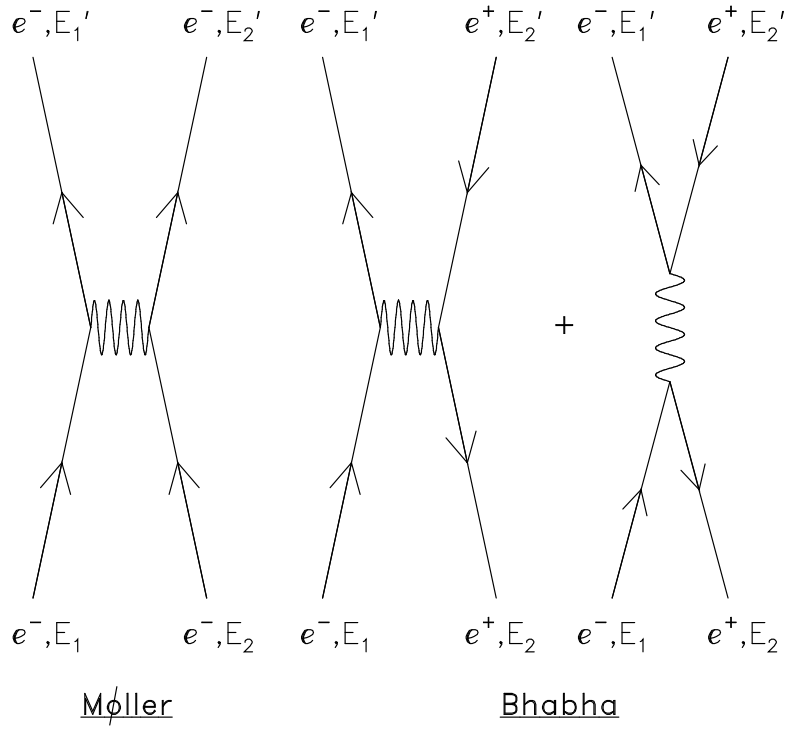

Figure 2: Feynman diagrams depicting the Møller and Bhabha interactions. Note the extra interaction channel in the case of the Bhabha interaction.

13.1.2 ... Møller (Bhabha) scattering...

Møller and Bhabha scattering are collisions of incident electrons or positrons with atomic electrons. It is conventional to assume that these atomic electrons are "free" ignoring their atomic binding energy. At first glance the Møller and Bhabha interactions appear to be quite similar. Referring to fig. 2, we see very little difference between them. In reality, however, they are, owing to the identity of the participant particles. The electrons in the e^-e^+ pair can annihilate and be recreated, contributing an extra interaction channel to the cross section. The thresholds for these interactions are different as well. In the e^-e^- case, the "primary" electron can only give at most half its energy to the target electron if we adopt the convention that the higher energy electron is always denoted "the primary". This is because the two electrons are indistinguishable. In the e^+e^- case the positron can give up all its energy to the atomic electron.

Møller and Bhabha cross sections scale with Z for different media. The cross section scales approximately as $1/v^2$, where v is the velocity of the scattered electron. Many more low energy secondary particles are produced from the Møller interaction than from the bremsstrahlung interaction.

13.1.3 Positron annihilation ...

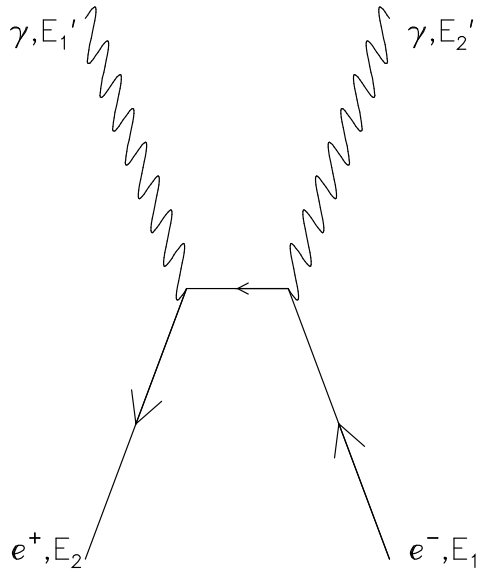

Annihilation

Figure 3: Feynman diagram depicting two-photon positron annihilation.

13.1.3 ... Positron annihilation

Two photon annihilation is depicted in fig. 3. Two-photon "in-flight" annihilation can be modeled using the cross section formulae of Heitler.

It is conventional to consider the atomic electrons to be free, ignoring binding effects. Three and higher-photon annihilations ($e^+e^- \longrightarrow n\gamma[n > 2]$) as well as one-photon annihilation which is possible in the Coulomb field of a nucleus ($e^+e^-\mathrm{N} \longrightarrow \gamma\mathrm{N}^*$) can be ignored as well.

The higher-order processes are very much suppressed relative to the two-body process (by at least a factor of $1/137$) while the one-body process competes with the two-photon process only at very high energies where the cross section becomes very small. If a positron survives until it reaches the transport cut-off energy it can be converted it into two photons (annihilation at rest), with or without modeling the residual drift before annihilation.

13.2 Statistically grouped interactions

13.2.1 "Continuous" energy loss ...

One method to account for the energy loss to sub-threshold (soft bremsstrahlung and soft collisions) is to assume that the energy is lost continuously along its path. The formalism that may be used is the Bethe-Bloch theory of charged particle energy loss as expressed by Berger and Seltzer and in ICRU 37.

This continuous energy loss scales with the Z of the medium for the collision contribution and Z^2 for the radiative part. Charged particles can also polarize the medium in which they travel. This "density effect" is important at high energies and for dense media. Default density effect parameters are available from a 1982 compilation by Sternheimer, Seltzer and Berger and state-of-the-art compilations (as defined by the stopping-power guru Berger who distributes a PC-based stopping power program).

Again, atomic binding effects are treated rather crudely by the Bethe-Bloch formalism. It assumes that each electron can be treated as if it were bound by an average binding potential. The use of more refined theories does not seem advantageous unless one wants to study electron transport below the K-shell binding energy of the highest atomic number element in the problem.

13.2.1 ... "Continuous" energy loss ...

The stopping power versus energy for different materials is shown in below.

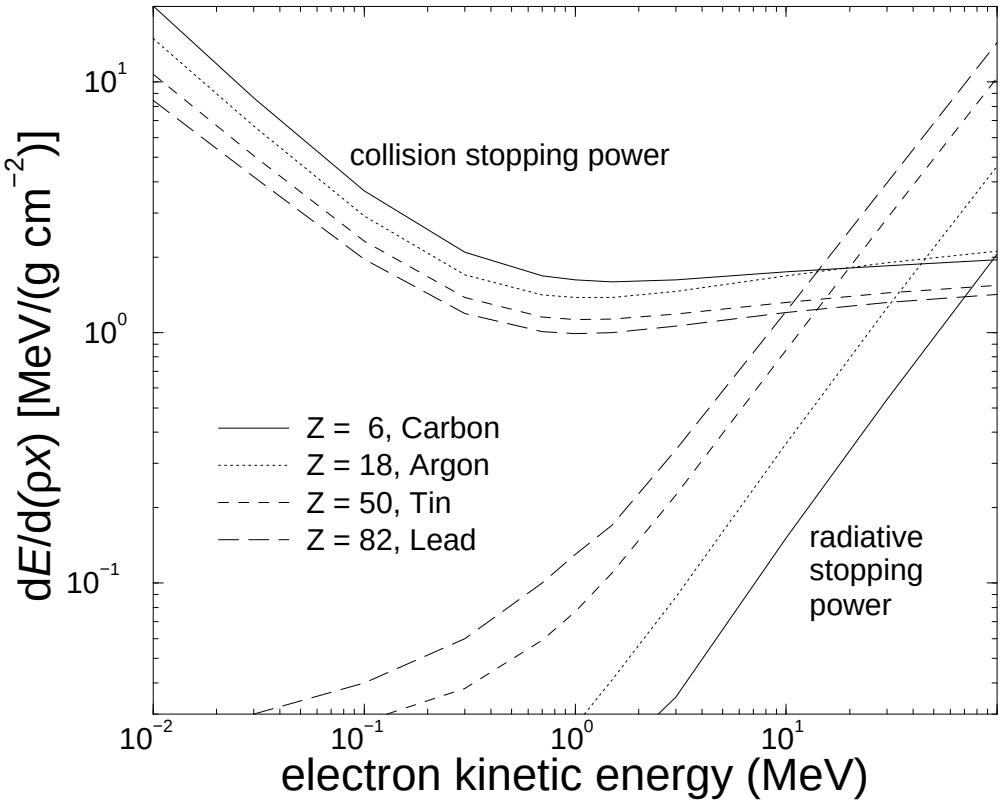

Figure 4: Stopping power versus energy.

13.2.1 ... "Continuous" energy loss ...

The difference in the collision part is due mostly to the difference in ionisation potentials of the various atoms and partly to a $\overline{Z}/\overline{A}$ difference, because the vertical scale is plotted in MeV/(g/cm^2), a normalisation by atomic weight rather than electron density. Note that at high energy the argon line rises above the carbon line. Argon, being a gas, is reduced less by the density effect at this energy. The radiative contribution reflects mostly the relative Z^2 dependence of bremsstrahlung production.

The collisional energy loss by electrons and positrons is different for the same reasons described in the "catastrophic" interaction section. Annihilation is generally not treated as part of the positron slowing down process and is treated discretely as a "catastrophic" event. The differences are reflected in fig. 5, the positron/electron collision stopping power.

13.2.1 ... "Continuous" energy loss ...

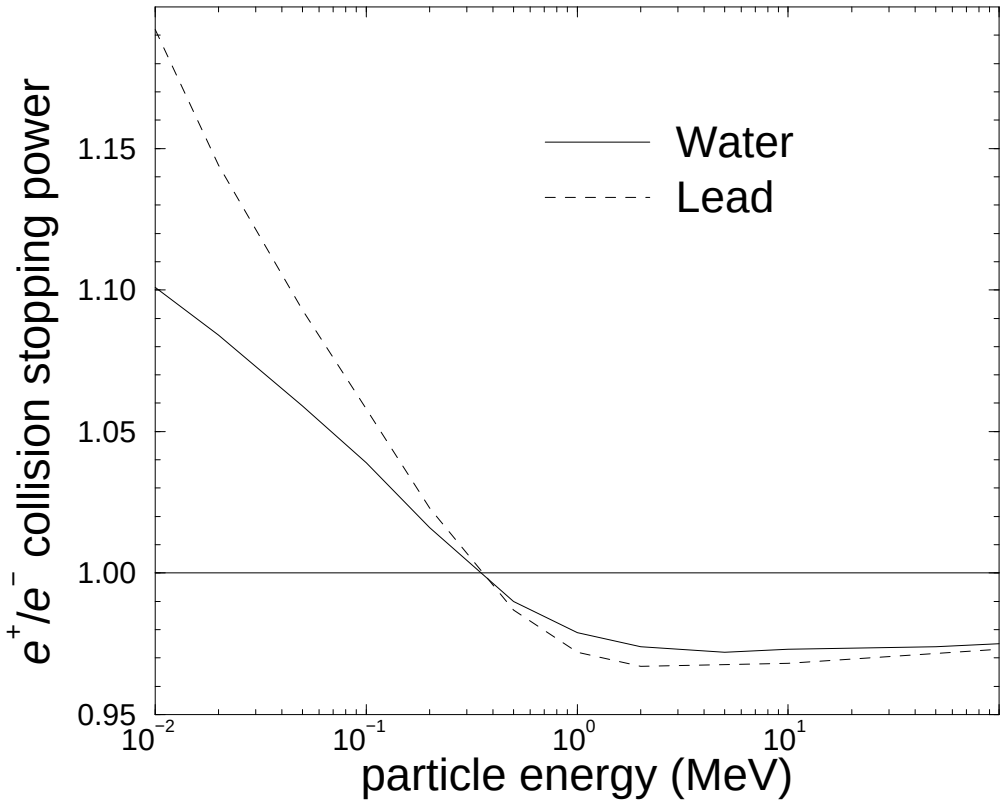

Figure 5: Positron/electron collision stopping power.

13.2.1 ... "Continuous" energy loss

The positron radiative stopping power is reduced with respect to the electron radiative stopping power. At 1 MeV this difference is a few percent in carbon and 60% in lead. This relative difference is depicted in below.

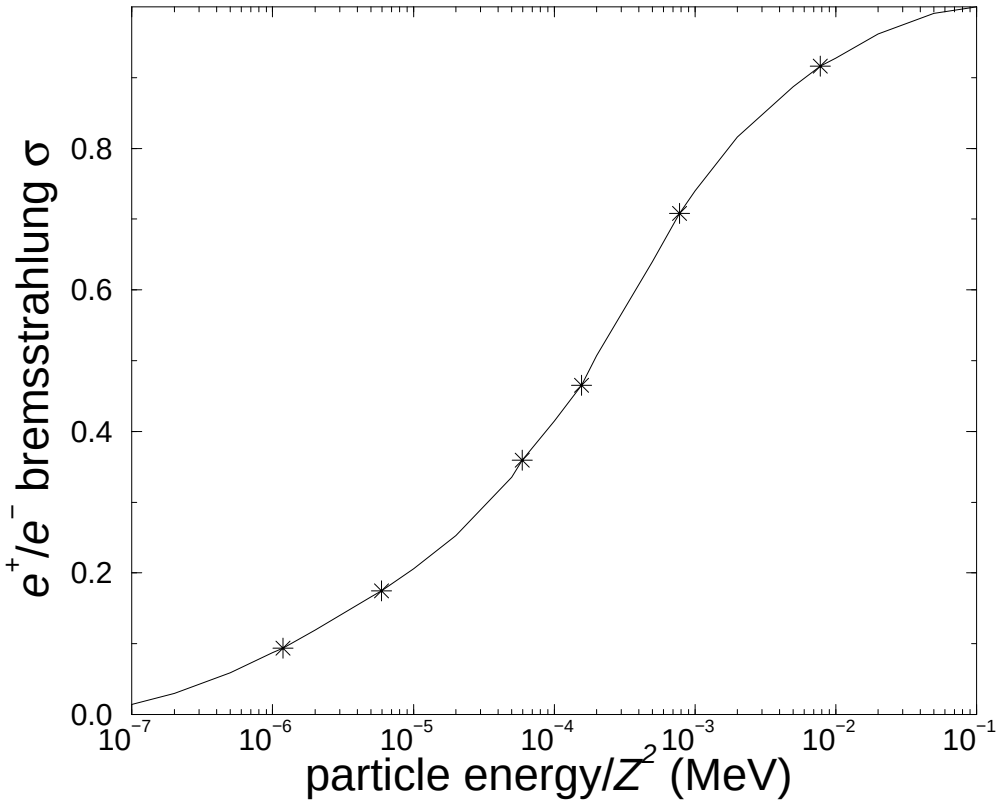

Figure 6: Positron/electron bremsstrahlung cross section.

13.2.2 Multiple scattering ...

Elastic scattering of electrons and positrons from nuclei is predominantly small angle with the occasional large-angle scattering event.

If it were not for screening by the atomic electrons, the cross section would be infinite.

The cross sections are, nonetheless, very large, essentially, the size of the atoms.

There are several statistical theories that deal with multiple scattering.

Some of these theories assume that the charged particle has interacted enough times so that these interactions may be grouped together.

Historically, the most popular such theory is the Fermi-Eyges theory, a small angle theory. This theory neglects large angle scattering and is unsuitable for accurate electron transport unless large angle scattering is somehow included (perhaps as a catastrophic interaction).

13.2.2 ... Multiple scattering ...

The most accurate theory is that of Goudsmit and Saunderson. This theory does not require that many atoms participate in the production of a multiple scattering angle. However, calculation times required to produce few-atom distributions can get very long, can have intrinsic numerical difficulties and are not efficient computationally for Monte Carlo codes such as EGS4 where the physics and geometry adjust the electron step-length dynamically.

A fixed step-size scheme permits an efficient implementation of Goudsmit-Saunderson theory and this has been done in ETRAN , ITS and MCNP.

EGS4 uses the Molière theory which produces results as good as Goudsmit-Saunderson for many applications and is much easier to implement in EGS4's transport scheme.

The Molière theory, although originally designed as a small angle theory has been shown with small modifications to predict large angle scattering quite successfully. The Molière theory includes the contribution of single event large angle scattering, for example, an electron backscatter from a single atom.

13.2.2 ... Multiple scattering ...

The Molière theory ignores differences in the scattering of electrons and positrons, and uses the screened Rutherford cross sections instead of the more accurate Mott cross sections. However, the differences are known to be small. Owing to analytic approximations made by Molière theory, this theory requires a minimum step-size as it breaks down numerically if less than 25 atoms or so participate in the development of the angular distribution. A recent development has surmounted this difficulty. Apart from accounting for energy loss, there is also a large step-size restriction because the Molière theory is couched in a small-angle formalism. Beyond this there are other corrections that can be applied related to the mathematical connection between the small-angle and any-angle theories.

13.3 Electron transport "mechanics"

13.3.1 Typical electron tracks ...

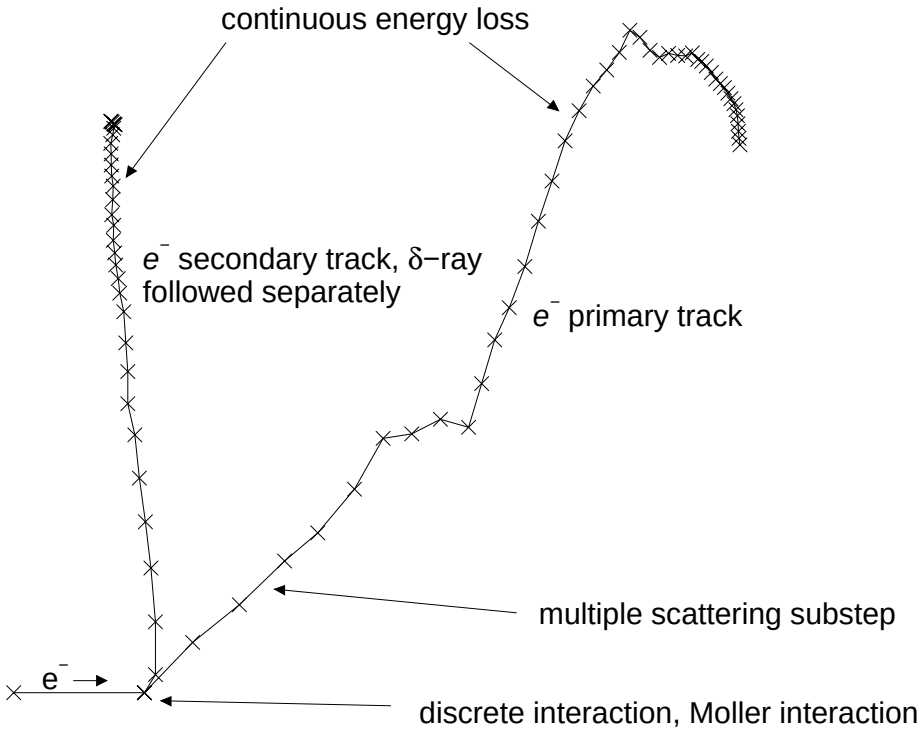

Figure 7: A typical electron track simulation. The vertical scale has been exaggerated somewhat.

13.3.1 ... Typical electron tracks

A typical Monte Carlo electron track simulation is shown in fig. 7. An electron is being transported through a scattering medium.

Along the way energy is being lost "continuously" to sub-threshold knock-on electrons and bremsstrahlung. The track is broken up into small straight-line segments called multiple scattering substeps.

In this case the length of these substeps was chosen so that the electron lost 4% of its energy during each step. At the end of each of these steps the multiple scattering angle is selected according to some theoretical distribution.

Catastrophic events, here a single knock-on electron, sets other particles in motion.

These particles are followed separately in the same fashion. The original particle, if it is does not fall below the transport threshold, is also transported.

In general terms, this is exactly what the electron transport logic simulates.

13.3.2 Typical multiple scattering substeps...

Now we demonstrate in fig. 8 what a multiple scattering substep should look like.

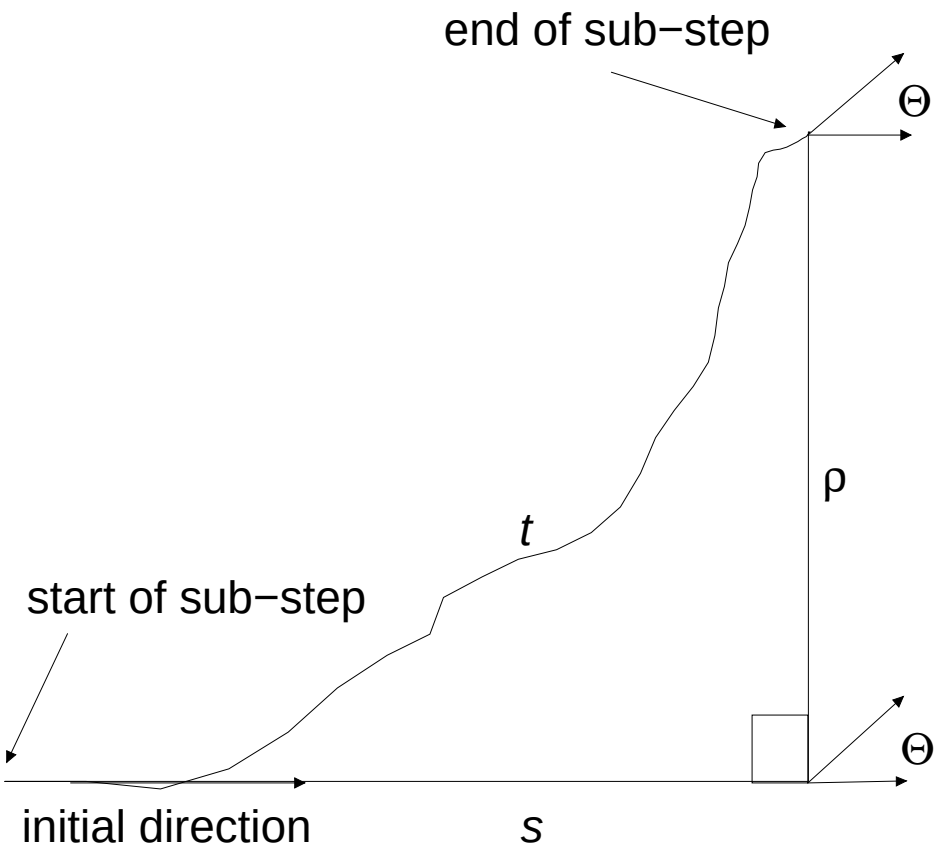

Figure 8: What a typical multiple scattering substep should look like.

13.3.2 ... Typical multiple scattering substeps...

A single electron step is characterized by the length of total curved path-length to the end point of the step, t.
(This is a reasonable parameter to use because the number of atoms encountered along the way should be proportional to t.)

At the end of the step the deflection from the initial direction, Θ, is sampled.

Associated with the step is the average projected distance along the original direction of motion, s.
(There is no satisfactory theory for the relation between s and t!)

The lateral deflection, ρ, the distance transported perpendicular to the original direction of motion, is often ignored by electron Monte Carlo codes. This is not to say that lateral transport is not modeled!

Recalling fig. 7, we see that such lateral deflections do occur as a result of multiple scattering. It is only the lateral deflection during the course of a substep which is ignored. One can guess that if the multiple scattering steps are small enough, the electron track may be simulated more exactly.

13.4 Examples of electron transport

13.4.1 Effect of physical modeling on a 20 MeV e^- depth-dose curve ...

In this section we will study the effects on the depth-dose curve of turning on and off various physical processes. Figure 9 presents two CSDA calculations (i.e. no secondaries are created and energy-loss straggling is not taken into account).

For the histogram, no multiple scattering is modeled and hence there is a large peak at the end of the range of the particles because they all reach the same depth before being terminating and depositing their residual kinetic energy (189 keV in this case). Note that the size of this peak is very much a calculational artefact which depends on how thick the layer is in which the histories terminate. The curve with the stars includes the effect of multiple scattering. This leads to a lateral spreading of the electrons which shortens the depth of penetration of most electrons and increases the dose at shallower depths because the fluence has increased. In this case, the depth-straggling is entirely caused by the lateral scattering since every electron has traveled the same distance.

13.4.1 ... Effect of physical modeling on a 20 MeV e^- depth-dose curve ...

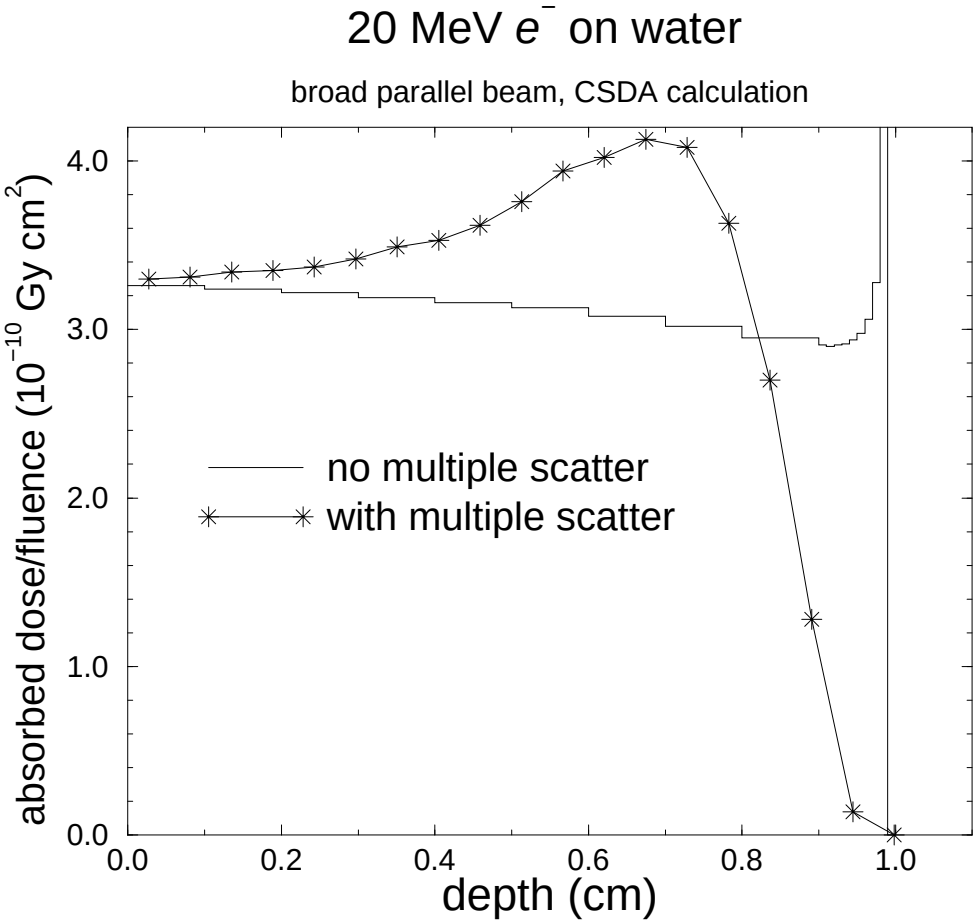

Figure 9: Depth-dose curve for a broad parallel beam (BPB) of 20 MeV electrons incident on a water slab. The histogram represents a CSDA calculation in which multiple scattering has been turned off, and the stars show a CSDA calculation which includes multiple scattering.

13.4.1 ... Effect of physical modeling on a 20 MeV e^- depth-dose curve ...

Figure 10 presents three depth-dose curves calculated with all multiple scattering turned off - i.e. the electrons travel in straight lines (except for some minor deflections when secondary electrons are created).

In the cases including energy-loss straggling, a depth straggling is introduced because the actual distance traveled by the electrons varies, depending on how much energy they give up to secondaries. Two features are worth noting. Firstly, the energy-loss straggling induced by the creation of bremsstrahlung photons plays a significant role despite the fact that far fewer secondary photons are produced than electrons. They do, however, have a larger mean energy. Secondly, the inclusion of secondary electron transport in the calculation leads to a dose buildup region near the surface. Figure 11 presents a combination of the effects in the previous two figures.

13.4.1 ... Effect of physical modeling on a 20 MeV e^- depth-dose curve ...

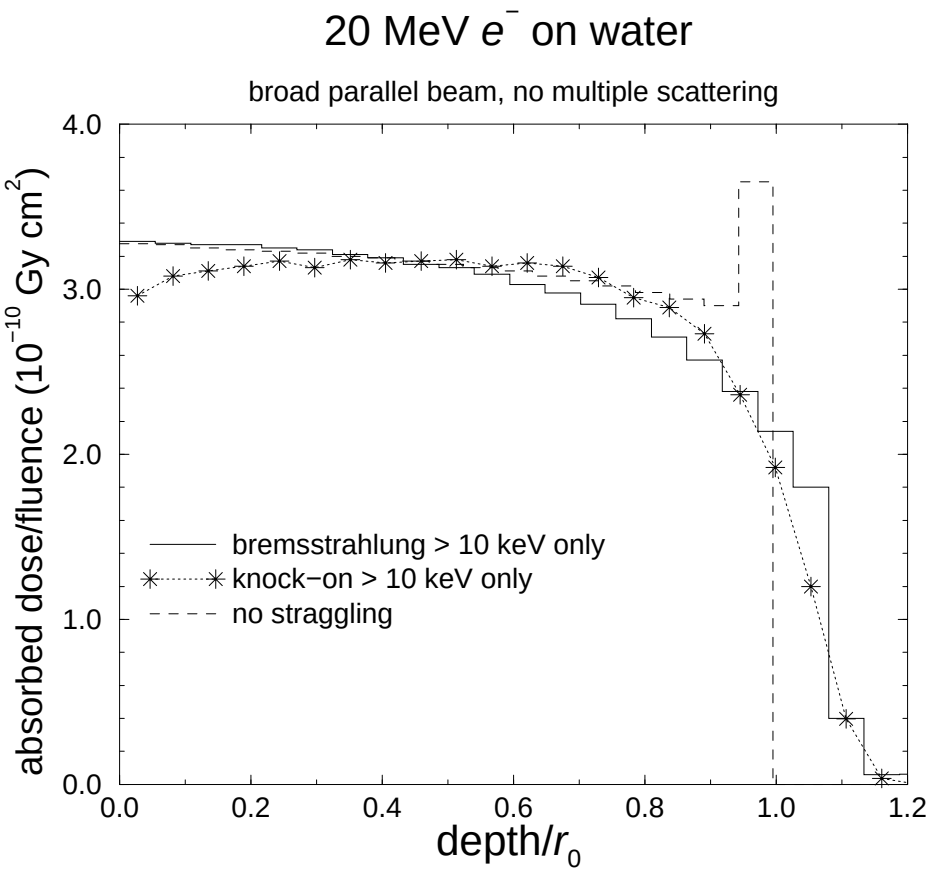

Figure 10: Depth-dose curves for a BPB of 20 MeV electrons incident on a water slab, but with multiple scattering turned off. The dashed histogram calculation models no straggling and is the same simulation as given by the histogram in fig. 9. Note the difference caused by the different bin size. The solid histogram includes energy-loss straggling due to the creation of bremsstrahlung photons with an energy above 10 keV. The curve denoted by the stars includes only that energy-loss straggling induced by the creation of knock-on electrons with an energy above 10 keV.

13.4.1 ... Effect of physical modeling on a 20 MeV e^- depth-dose curve ...

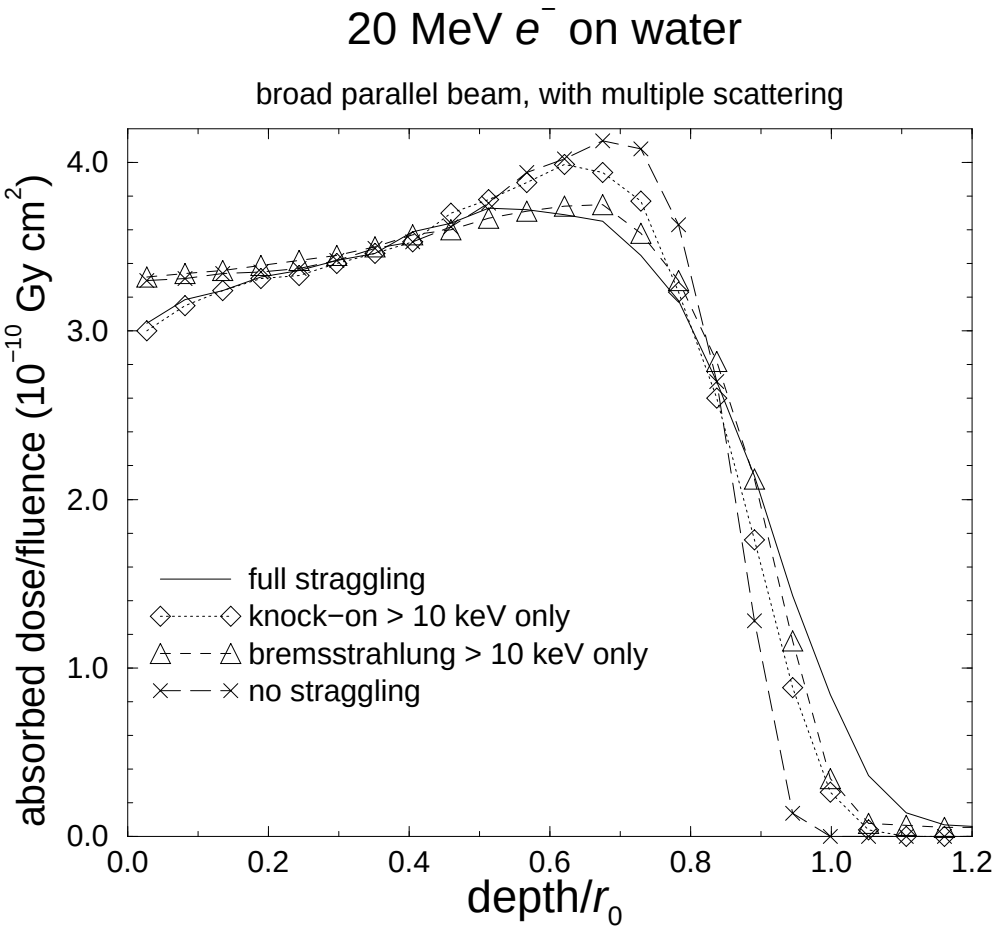

Figure 11: BPB of 20 MeV electrons on water with multiple scattering included in all cases and various amounts of energy-loss straggling included by turning on the creation of secondary photons and electrons above a 10 keV threshold.

13.4.1 ... Effect of physical modeling on a 20 MeV e^- depth-dose curve

The extremes of no energy-loss straggling and the full simulation are shown to bracket the results in which energy-loss straggling from either the creation of bremsstrahlung or knock-on electrons is included. The bremsstrahlung straggling has more of an effect, especially near the peak of the depth-dose curve.

13.5 Electron transport logic ...

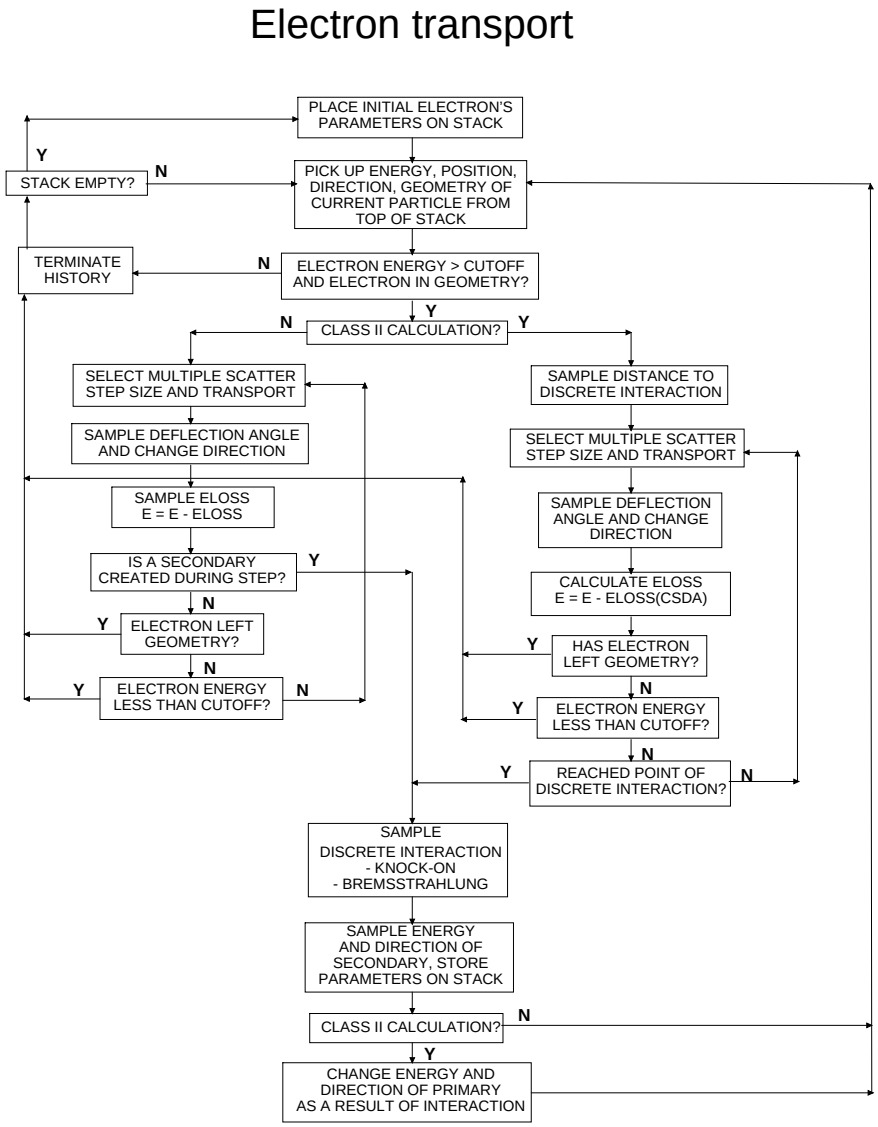

Figure 12: Flow chart for electron transport. Much detail is left out.

13.5 ... Electron transport logic ...

Figure 12 is a schematic flow chart showing the essential differences between different kinds of electron transport algorithms. EGS4 is a "class II" algorithm which samples interactions discretely and correlates the energy loss to secondary particles with an equal loss in the energy of the primary electron (positron).

There is a close similarity between this flow chart and the photon transport flow chart. The essential differences are the nature of the particle interactions as well as the additional continuous energy-loss mechanism and multiple scattering. Positrons are treated by the same subroutine in EGS4 although it is not shown in fig. 12.

Imagine that an electron's parameters (energy, direction, etc.) are on top of the particle stack. (`STACK` is an array containing the phase-space parameters of particles awaiting transport.) The electron transport routine, picks up these parameters and first asks if the energy of this particle is greater than the transport cutoff energy, called `ECUT`. If it is not, the electron is discarded. (This is not to that the particle is simply thrown away! "Discard" means that the scoring routines are informed that an electron is about to be taken off the transport stack.) If there is no electron on the top of the stack, control is given to the photon transport routine. Otherwise, the next electron in the stack is picked up and transported.

13.5 ... Electron transport logic

If the original electron's energy was great enough to be transported, the distance to the next catastrophic interaction point is determined, exactly as in the photon case. The multiple scattering step-size t is then selected and the particle transported, taking into account the constraints of the geometry.

After the transport, the multiple scattering angle is selected and the electron's direction adjusted. The continuous energy loss is then deducted. If the electron, as a result of its transport, has left the geometry defining the problem, it is discarded. Otherwise, its energy is tested to see if it has fallen below the cutoff as a result of its transport. If the electron has not yet reached the point of interaction a new multiple scattering step is effected. This innermost loop undergoes the heaviest use in most calculations because often many multiple scattering steps occur between points of interaction (see fig. 7). If the distance to a discrete interaction has been reached, then the type of interaction is chosen. Secondary particles resulting from the interaction are placed on the stack as dictated by the differential cross sections, lower energies on top to prevent stack overflows. The energy and direction of the original electron are adjusted and the process starts all over again.